Supplement of Earth Syst. Dynam., 17, 987–1006, 2026
https://doi.org/10.5194/esd-17-987-2026-supplement

Supplement of

Amplification of ENSO-driven vegetation variability at decadal and longer timescales

Nora L. S. Fahrenbach and Robert C. J. Wills

Correspondence to: Nora L. S. Fahrenbach (nora.fahrenbach@env.ethz.ch)

S1 Regression of LAI on Niño3.4 index for individual models

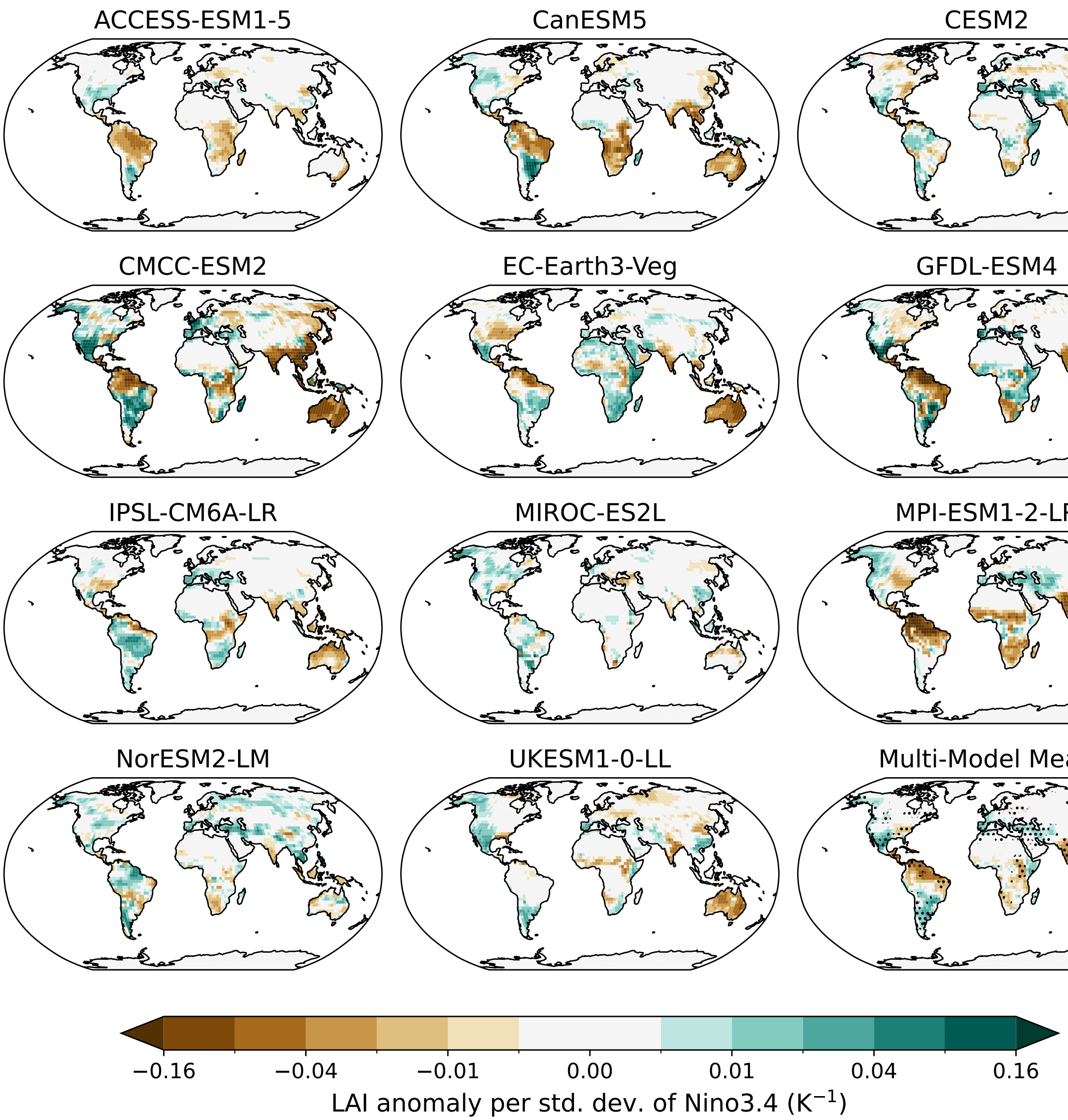

Figure S1. Spatial map of seasonal LAI anomalies regressed on the seasonal Niño3.4 index, normalized by the standard deviation of the Niño3.4 index, for each individual CMIP6 model used in this study and the MEM. The analysis uses 500 years of CMIP6 piControl simulations. Stippling in the MEM plot indicates agreement on the sign of change by at least 9 out of 11 models (90% confidence).

S2 Gridcell-level coherence and gain analysis

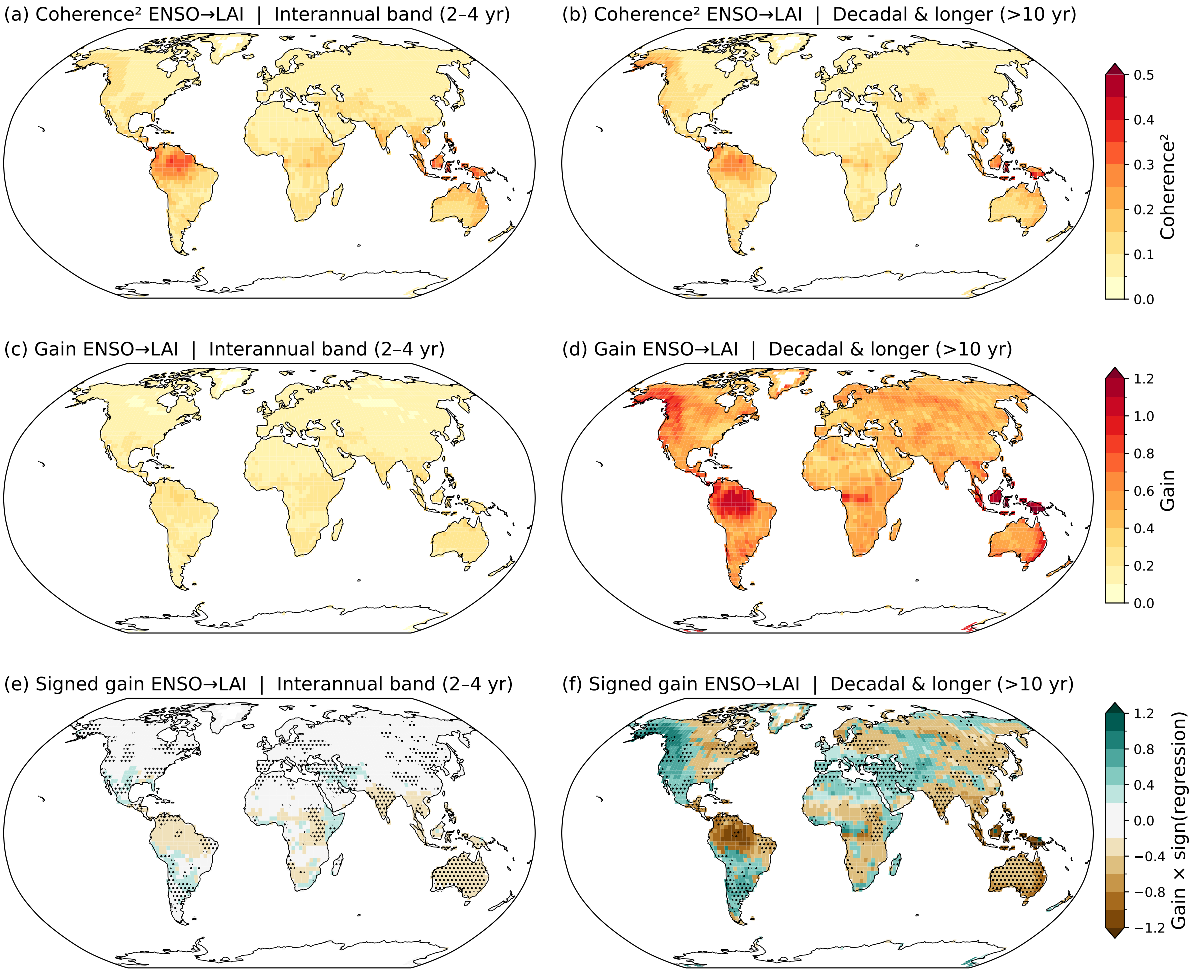

Figure S2. Gridcell-level MEM of (a, b) coherence squared and (c, d) gain magnitude between the Niño3.4 index and LAI in piControl, evaluated in the (left column) interannual 2–4 yr period band and (right column) decadal-and-longer > 10 yr period. Subplots (e, f) show the gain magnitude multiplied by the sign of the MEM regression coefficient (Fig. 3a), so that negative (brown) and positive (green) vegetation anomaly hotspots can be distinguished. Stippling in (e, f) indicates where at least 9 of the 11 models agree on the sign of the regression. LAI at each grid cell is standardised by its local standard deviation prior to the spectral analysis, so the gain values are directly comparable to the global Tv gain in Fig. 3d.

S3 Regional coherence analysis

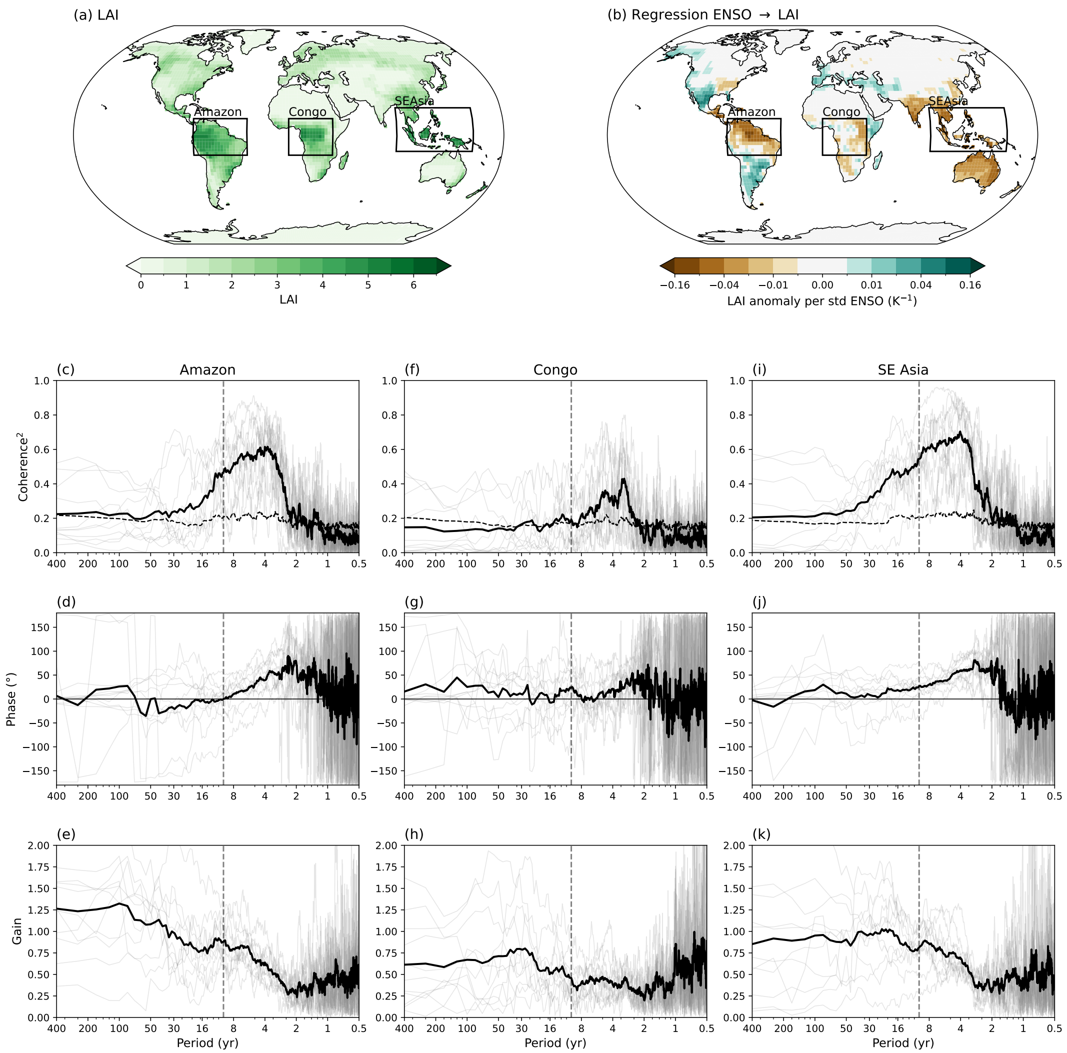

Figure S3. Maps of multi-model mean piControl (a) leaf area index and (b) seasonal LAI anomalies regressed on the seasonal Niño3.4 index. (c-k) Coherence squared, phase, and gain between the Niño3.4 index and LAI regressed on Niño3.4 in piControl over the (c-e) Amazon, (f-h) Congo and (i-k) Southeast Asian rainforest regions. Boxes in (a) and (b) show the regions used for the regional spectral analysis in (c-k). Note that while the choice of fixed geographic regions allows spatial comparability, it might obscure some model-specific teleconnection patterns. The black dashed line in panels (a, f, i) show the critical coherence squared at the 90% significance level. The dashed vertical lines in (c-k) mark a period of 10 years.

S4 Coherence analysis between ENSO and PDO

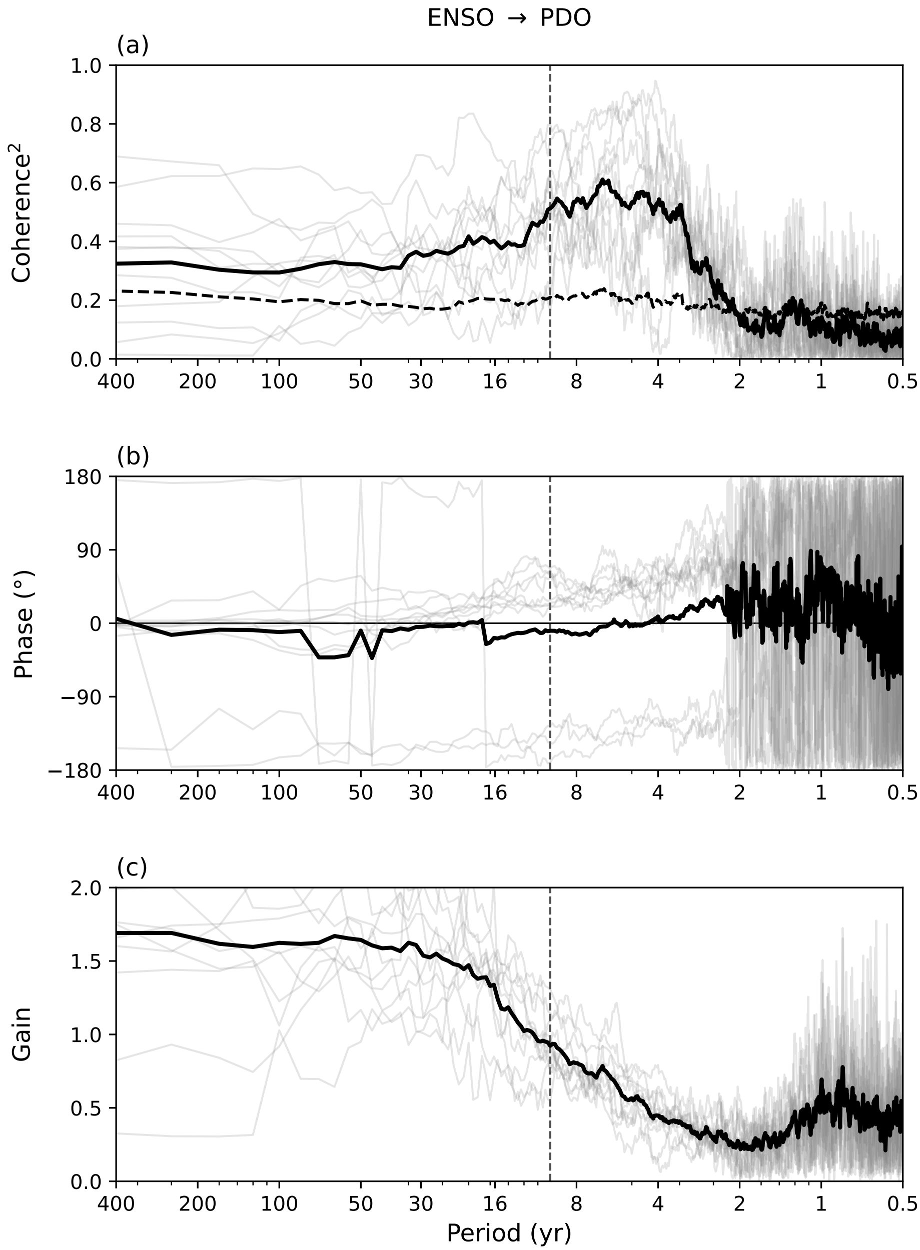

Figure S4. Coherence squared, phase, and gain between the Niño3.4 index and the PDO index, calculated from 500 years of CMIP6 piControl simulations. The thick line represents the MEM, and thin lines show individual model results. The black dashed line in panel (a) shows the critical coherence squared at the 90% significance level. The dashed vertical lines mark a period of 10 years.

S5 Coherence analysis between AMV and LAI

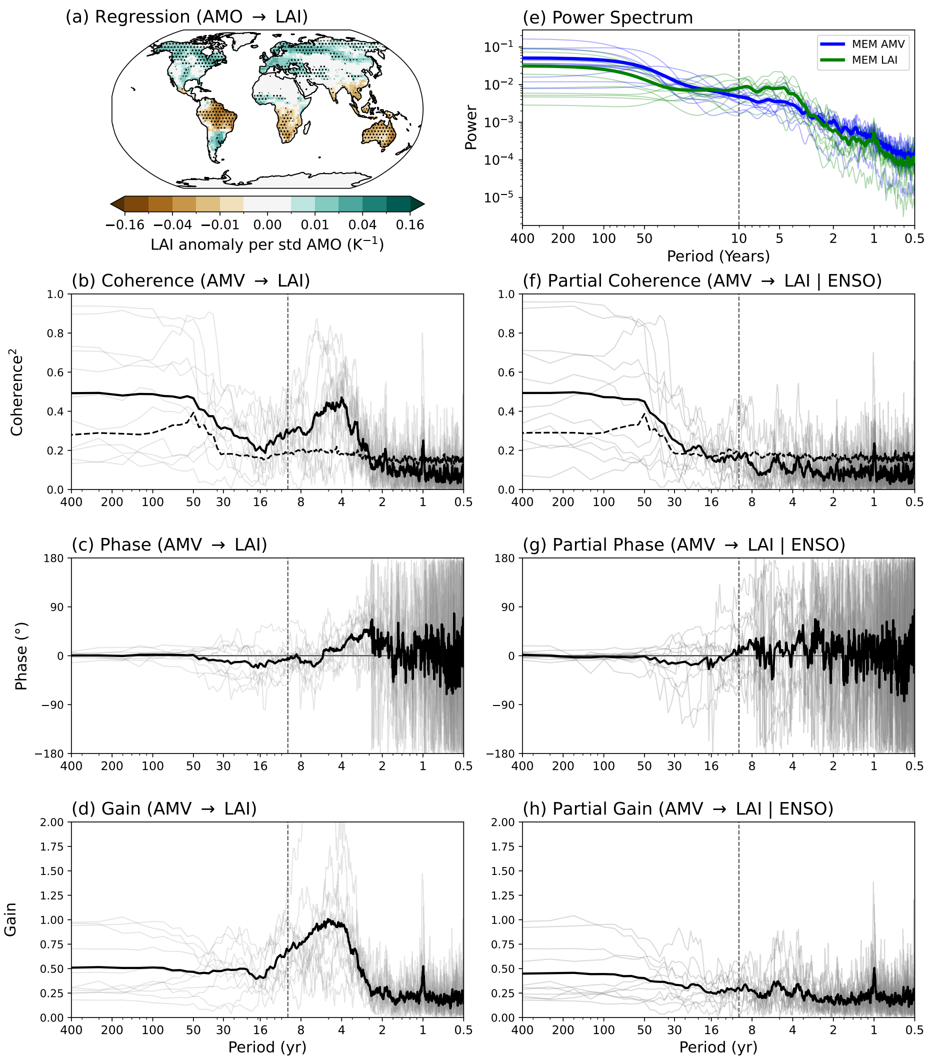

Figure S5. (a) Spatial map of the MEM regression coefficient of seasonal LAI anomalies on the AMV index, normalized by the standard deviation of the AMV index. The regression coefficient is calculated for each model based on 500 years of linearly detrended CMIP6 piControl simulations. Stippling indicates agreement on the sign of change by at least 9 of the 11 models (90% confidence). (b-d) Coherence squared, phase, and gain between the AMV index and LAI regressed on AMV in piControl. (e) Power spectrum of the AMV index (thick blue line for MEM, thin blue lines for individual models) and LAI regressed on AMV (thick green line for the MEM, thin green lines for individual models) in piControl. (f-h) Partial coherence squared, phase, and gain between the AMV index and LAI regressed on AMV in piControl, with the linear influence of the Niño3.4 index removed. In panels (b-d) and (f-h), the thick black line represents the MEM mean, and thin grey lines show individual model results. The black dashed lines in panels (b) and (f) show the critical coherence squared at the 90% significance level. The dashed vertical lines in panels (b-h) mark a period of 10 years.

S6 Coherence analysis between ENSO and LAI without net precipitation and temperature influence

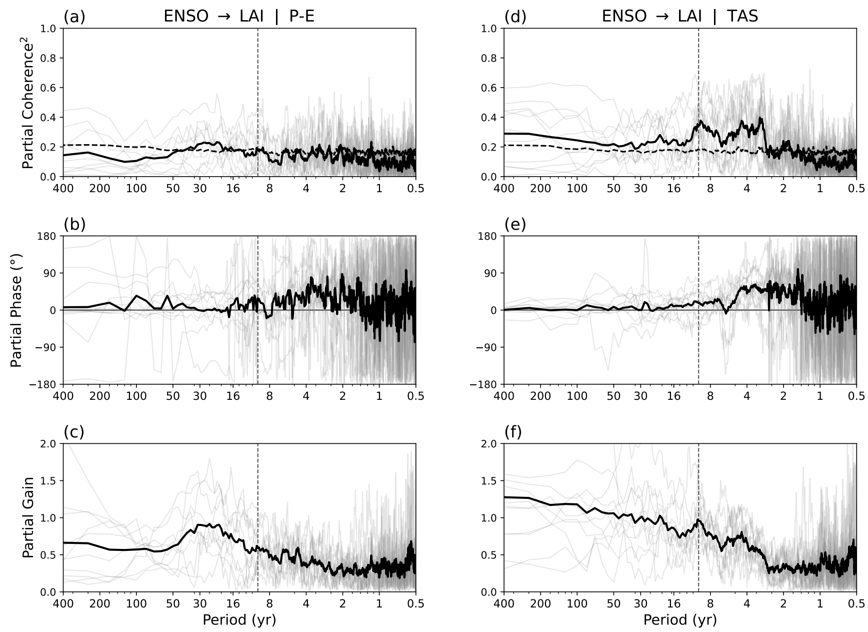

Figure S6. Partial coherence squared, phase, and gain between the Niño3.4 index and LAI regressed on Niño3.4, with the linear influence of (a-c) net precipitation (precipitation P minus evapotranspiration E) and (d-f) near-surface air temperature (TAS) excluded. The thick line represents the MEM, and thin lines show individual model results. The black dashed line in panel (a, d) shows the critical coherence squared at the 90% significance level. The dashed vertical lines mark a period of 10 years.

S7 Regression of GPP on Niño3.4 index for individual models

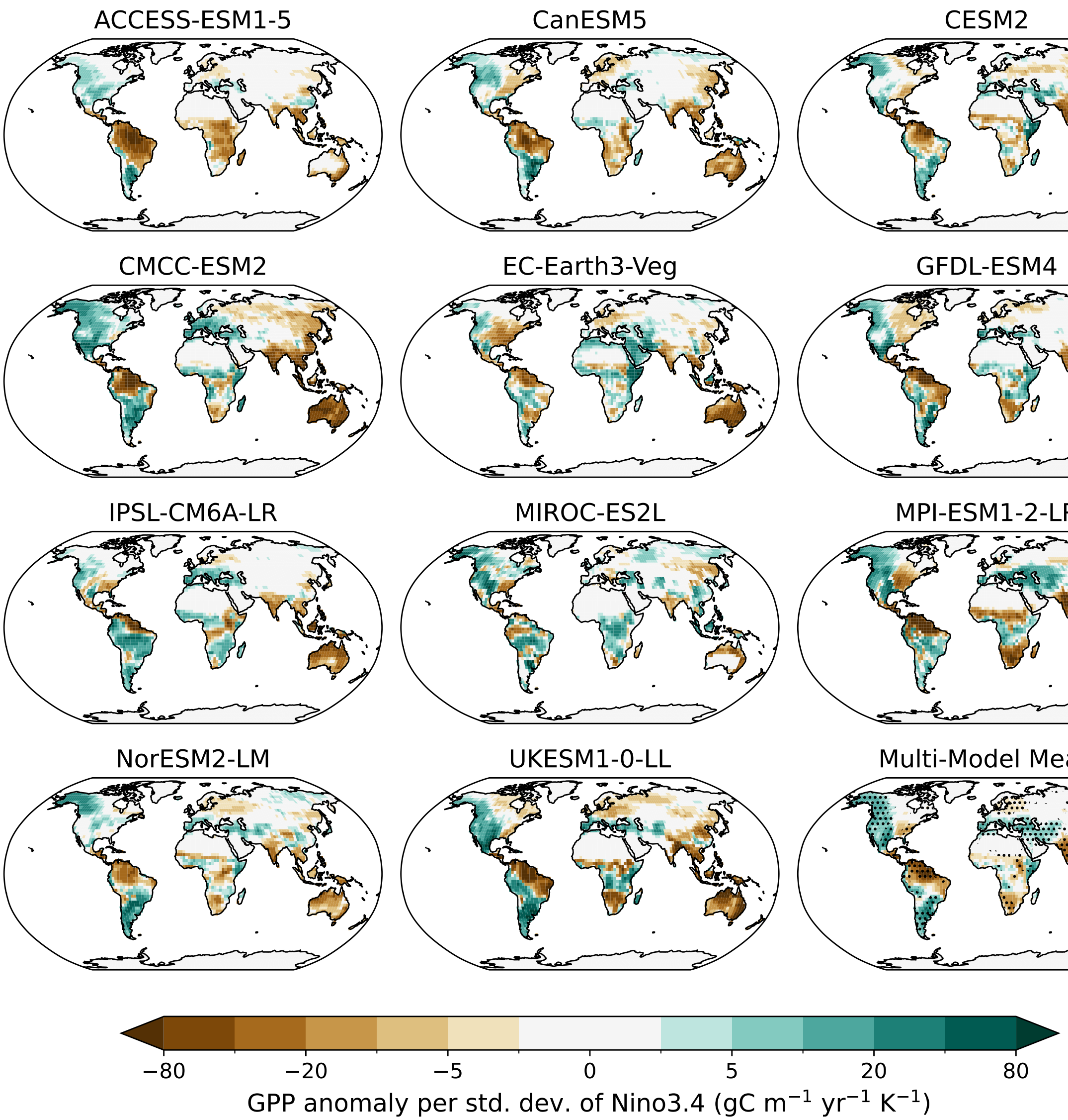

Figure S7. Spatial map of seasonal anomalies in GPP regressed on the Niño3.4 index, normalized by the standard deviation of the Niño3.4 index, for each individual CMIP6 model used in this study and the MEM. The analysis uses 500 years of CMIP6 piControl simulations. Stippling in the MEM plot indicates agreement on the sign of change by at least 9 out of 11 models (90% confidence).

S8 Regression of NPP on Niño3.4 index for individual models

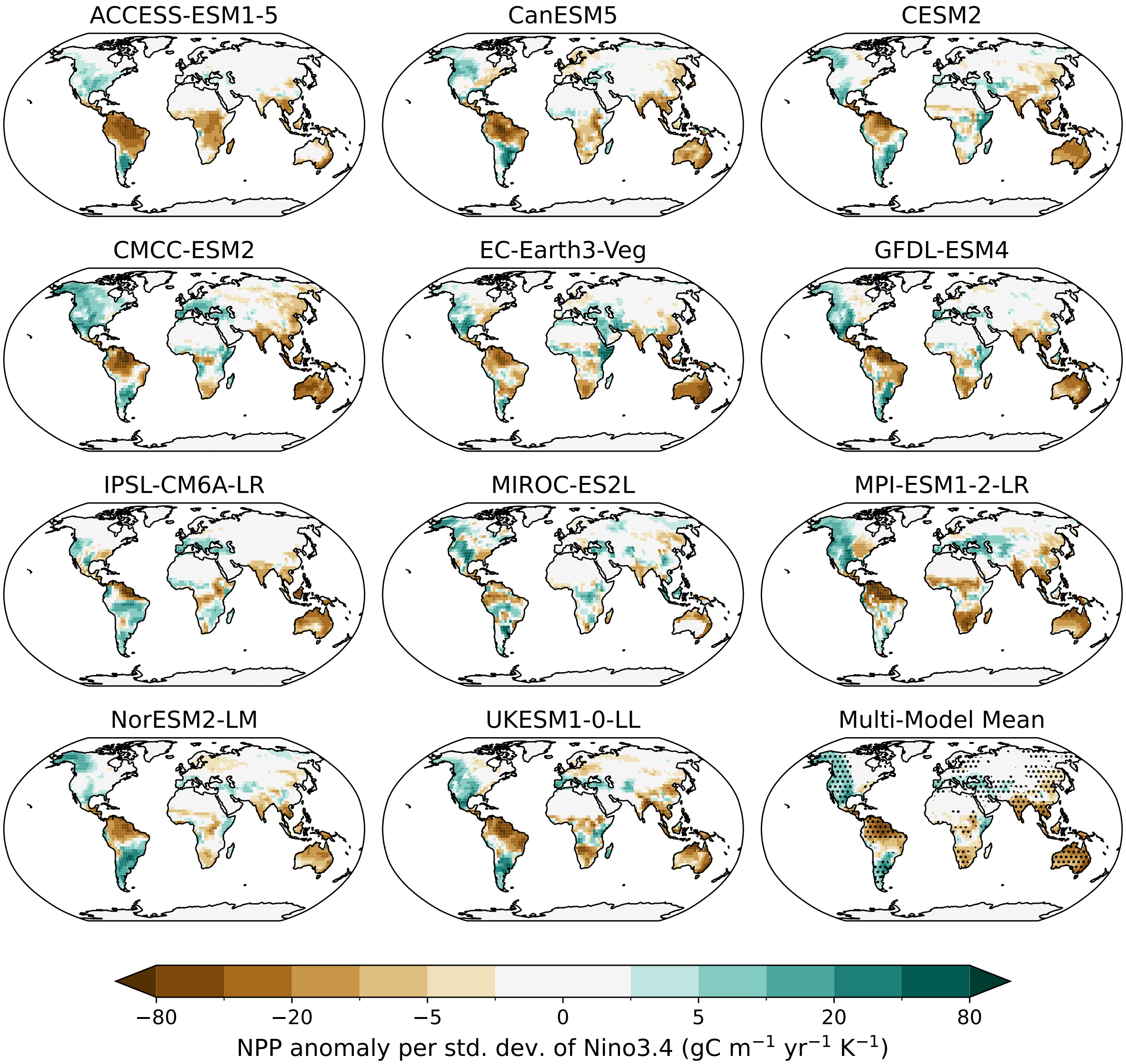

Figure S8. Spatial map of seasonal anomalies in NPP regressed on the Niño3.4 index, normalized by the standard deviation of the Niño3.4 index, for each individual CMIP6 model used in this study and the MEM. The analysis uses 500 years of CMIP6 piControl simulations. Stippling in the MEM plot indicates agreement on the sign of change by at least 9 out of 11 models (90% confidence).

S9 Coherence of GPP and autotrophic respiration

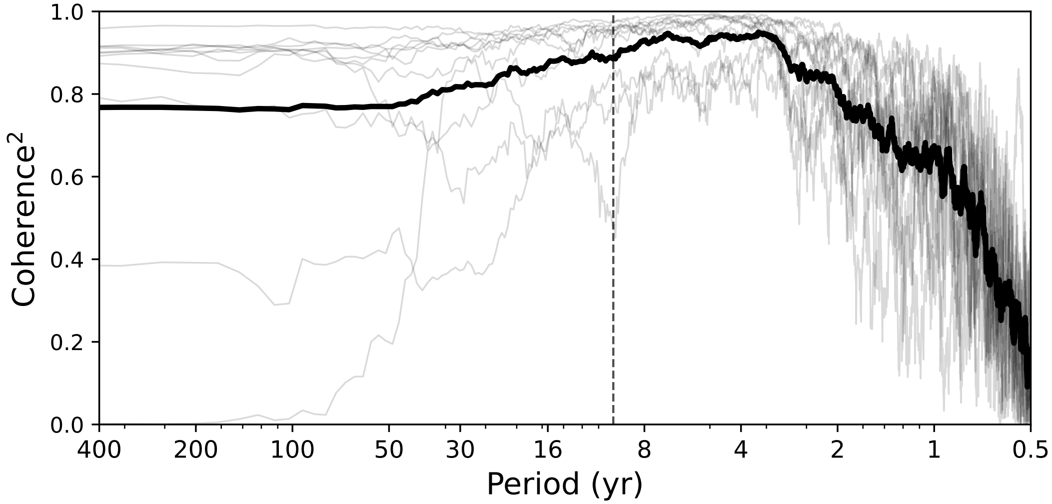

Figure S9. Coherence squared of GPP regressed on Niño3.4 and autotrophic respiration (R_a) regressed on Niño3.4 for the multi-model mean MEM (black thick line) and individual models (thin black lines). The dashed vertical line marks a period of 10 years.

S10 Coherence analysis between ENSO and LAI for historical CMIP6 and observations

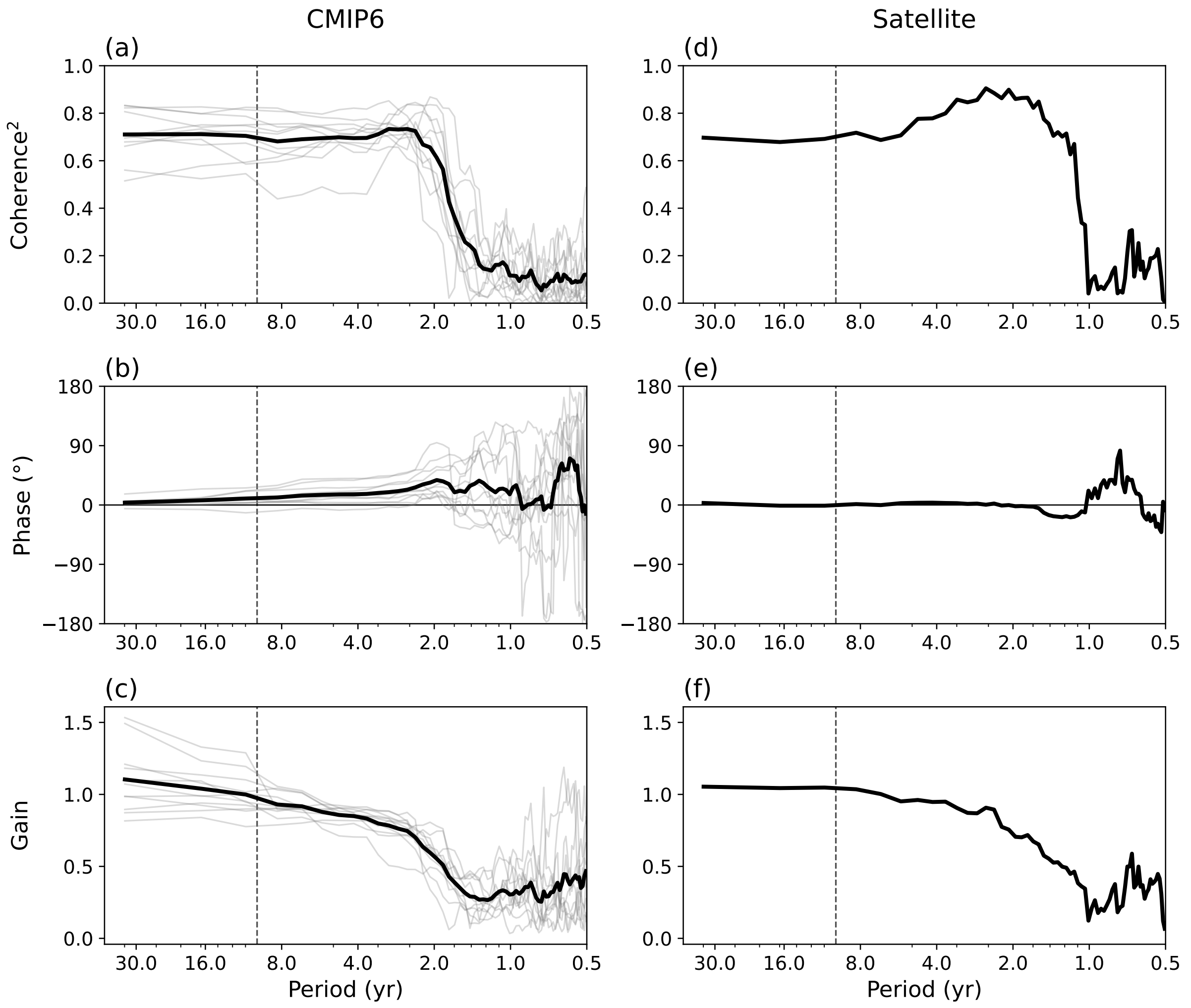

Figure S10. Coherence squared, phase, and gain of the Niño3.4 index and LAI regressed on Niño3.4 for the historical period 1980–2014. (a-c) show results using CMIP6 historical simulation data, where thin grey lines represent individual models and the thick black line shows the MEM. (d-f) show results using HadISST SST for the Niño3.4 index and GLASS LAI. The dashed vertical lines mark a period of 10 years.